Integrative and Comparative Biology

Integrative and Comparative Biology, volume 61, number 5, pp. 1644–1657
doi:10.1093/icb/icab119

Society for Integrative and Comparative Biology

SYMPOSIUM

Dual Phase-Shifted Ipsilateral Metachrony in *Americamysis bahia*

Melissa Ruszczyk,[1,*] Donald R. Webster[†] and Jeannette Yen [‡]

*Ocean Science and Engineering, Georgia Institute of Technology, Atlanta, GA 30332, USA; [†]Civil and Environmental Engineering, Georgia Institute of Technology, Atlanta, GA 30332, USA; [‡]Biological Sciences, Georgia Institute of Technology, Atlanta, GA 30332, USA

From the Symposium "Metachronal Coordination of Multiple Appendages for Swimming and Pumping" Presented at the Virtual Annual Meeting of the Society for Integrative and Comparative Biology, January 3–7, 2020.

[1]E-mail: mruszczyk3@gatech.edu

Synopsis Previously documented metachrony in euphausiids focused on one, five-paddle metachronal stroke, where contralateral pleopod pairs on the same abdominal segment beat in tandem with each other, propelling the animal forward. In contrast, the mysid shrimp *Americamysis bahia*'s pleopods on the same abdominal segment beat independently of each other, resulting in two, five-paddle metachronal cycles running ipsilaterally along the length of the body, 180° out of phase. The morphology, kinematics, and nondimensional measurements of efficiency are compared primarily with the one-cycle *Euphausia superba* to determine how the two-cycle approach alters the design and kinematics of metachrony. Pleopodal swimming in *A. bahia* results in only fast-forward swimming, with speeds greater than 2 BL/s (body lengths per second), and can reach speeds up to 12 BL/s, through a combination of increasing stroke amplitude, increasing beat frequency, and changing their inter-limb phase lag. Trends with Strouhal number and advance ratio suggest that the kinematics of metachrony in *A. bahia* are favored to achieve large normalized swimming speeds.

Introduction

One aspect of an organism's physical environment that plays a role in their propulsive design is the relative importance of viscous effects compared with inertial effects. The Reynolds number (Re), calculated as

$$\mathrm{Re} = \frac{\rho UL}{\mu} = \frac{UL}{\nu}, \quad (1)$$

where ρ is the fluid density, U is the characteristic velocity, L is the characteristic length of the object, μ is the dynamic viscosity of the fluid, and ν is the kinematic viscosity, is a nondimensional parameter that characterizes the balance between viscous and inertial forces. At high Reynolds numbers ($\mathrm{Re} \gg 1000$), inertial forces dominate, and at lower Reynolds numbers ($\mathrm{Re} \ll 1$), viscous forces dominate. Contending with different force balances results in different approaches to propulsion in organisms (Yen 2000), which is perhaps best observed in aquatic environments.

At high Reynolds numbers ($\mathrm{Re} \gg 1000$), aquatic propulsion occurs as the result of flapping via appendages, such as flippers or fins, or undulating motions, like rays, in a plane perpendicular to the direction of movement, generating thrust through vortex shedding (Vogel 2013). Fish, rays, and aquatic mammals such as whales, dolphins, and porpoises utilize lift-based propulsion to swim (Drucker and Jensen 1996; Fish and Lauder 2006; Fulton et al. 2013; Ayancik et al. 2020).

At lower Reynolds numbers ($\mathrm{Re} \ll 1000$), there are two distinct approaches to propulsion. In jetting, organisms, such as jellyfish (DeMont and Gosline 1988), siphonophores (Costello et al. 2015), and squids (Anderson and Grosenbaugh 2005), contract and expel a jet of fluid in the direction opposite of motion. In drag-based propulsion, appendage motion occurs in a plane parallel to the direction of motion, like a paddle. It consists of a power stroke in which the appendage is fully extended, and a recovery stroke in which the appendage contracts.

Advance Access publication 3 June 2021

Bristles or hairs may fan out during the power stroke and retract on the recovery stroke, causing the limb to function as a "leaky rake" in parts of the stroke (Cheer and Koehl 1987). This causes the surface area to vary throughout the stroke, resulting in greater drag during the power stroke and ultimately a net forward thrust force (Kim and Gharib 2011). The pressure distribution around the appendage also plays a key role in determining the thrust generated (Colin et al. 2020).

Crustaceans have different approaches to drag-based propulsion, making them an ideal group to investigate overarching design elements for these propulsive systems. The first design element to consider in drag-based propulsion is the number of paddles used in the stroke. This number is highly variable within crustaceans, ranging from 2 in the daphniid *Daphnia magna* (Skipper et al. 2019), to 38 in the remipede *Speleonectes lucayensis* (Kohlhage and Yager 1994). A second design element is paddle orientation. Paddles may be positioned in a monoplanar arrangement (euphausiid pleopods, Murphy et al. 2011) or in two parallel planes that vary during the power and recovery strokes to minimize appendage congestion (remipede legs, Kohlhage and Yager 1994; mysid thoracopods, Laverack et al. 1977). A third design element to consider is paddle synchrony. Adjacent appendages may beat independently of each other or at the same time. In euphausiids, contralateral—left and right—pleopods beat at the same time. Although they have 10 total appendages, this results in a five-paddle stroke. Additionally, paddles may undergo their power and recovery strokes at the same time resulting in a synchronous stroke, or beat with a phase difference among paddles. When the paddles stroke in an adlocomotory, time-delayed manner, the stroke is metachronal. A complete stroke, consisting of both the power and recovery stroke, may be completely synchronous (daphniids, Skipper et al. 2019), completely metachronal (euphausiids, Alben et al. 2010; Murphy et al. 2011), or a combination of synchronous and metachronal (*Odontodactylus havanensis* escape response, Campos et al. 2012). There is also variability between each paddle. By changing parameters such as stroke amplitude, beat frequency, and time delay between adjacent power strokes, *Euphausia superba* achieves a variety of different swimming styles (Murphy et al. 2011, 2013). Further, morphological parameters, including the distance between paddles and the paddle shape, add more variables to the design space.

Data from these observational studies have been applied in models and experimental systems to determine the optimal parameters of a metachronal stroke and how parameters vary with Reynolds number. By altering the time delay between power strokes of adjacent paddles, studies have shown that perfect metachrony—having the same phase delay between all adjacent paddles—results in the greatest body speeds (Alben et al. 2010; Ford and Santhanakrishnan 2020) and greatest efficiency measured by fluid flux per stroke (Zhang et al. 2014; Granzier-Nakajima et al. 2020). Models also predict that the number of paddles needed to maximize distance traveled per unit energy varies with Reynolds number (Granzier-Nakajima et al. 2020). However, these models only account for the organism having one metachronal cycle occurring at a time. How would these parameters change if an organism were to have multiple concurrent metachronal cycles?

Mysid shrimp (superorder Paracarida) are malacostracan crustaceans with a similar, shrimp-like body plan to euphausiids, known as the caridoid facies. Mysids are distinguishable from other malacostracans by the presence in females of a brood pouch, or marsupium, on the base of their thoracic appendages, thoracopods, where they keep fertilized eggs until they hatch (Fig. 1A). In contrast, many euphausiids, including *E. superba* and *Euphausia pacifica* are broadcast spawners and release gametes into the water, thus they lack a marsupium (Ross and Quetin 2000). Additionally, euphausiids and decapods, which use their pleopods to swim, have a structure called a retinaculum on their pleopods that function as a set of hooks, linking the pleopods on the same abdominal segment together and ensuring that they beat in tandem. Mysid shrimp do not have a retinaculum, allowing pleopods on the same abdominal segment to move independently of each other, doubling the number of paddles the mysid uses in its metachronal stroke (Grams and Richter 2021).

Pleopod morphology and the resulting propulsive approach differs among the three orders of mysid shrimp. Stygiomysida pleopods are reduced and these mysids rely solely on their thoracopods for swimming (Meland et al. 2015). In contrast, Lophogastrida, such as *Gnathophausia ingens*, have five fully-developed pleopod pairs that beat with eight thoracopod pairs in a metachronal stroke comprised of two antiphase cycles (Hessler 1985; Quetin and Childress 1980). Mysida propulsion is less well-defined. Early sources claim that Mysida pleopods are small, rudimentary, and not used for swimming (Tattersall and Tattersall 1951), though more recent sources claim that, depending on the species, male Mysida have fully-developed, biramous pleopods that

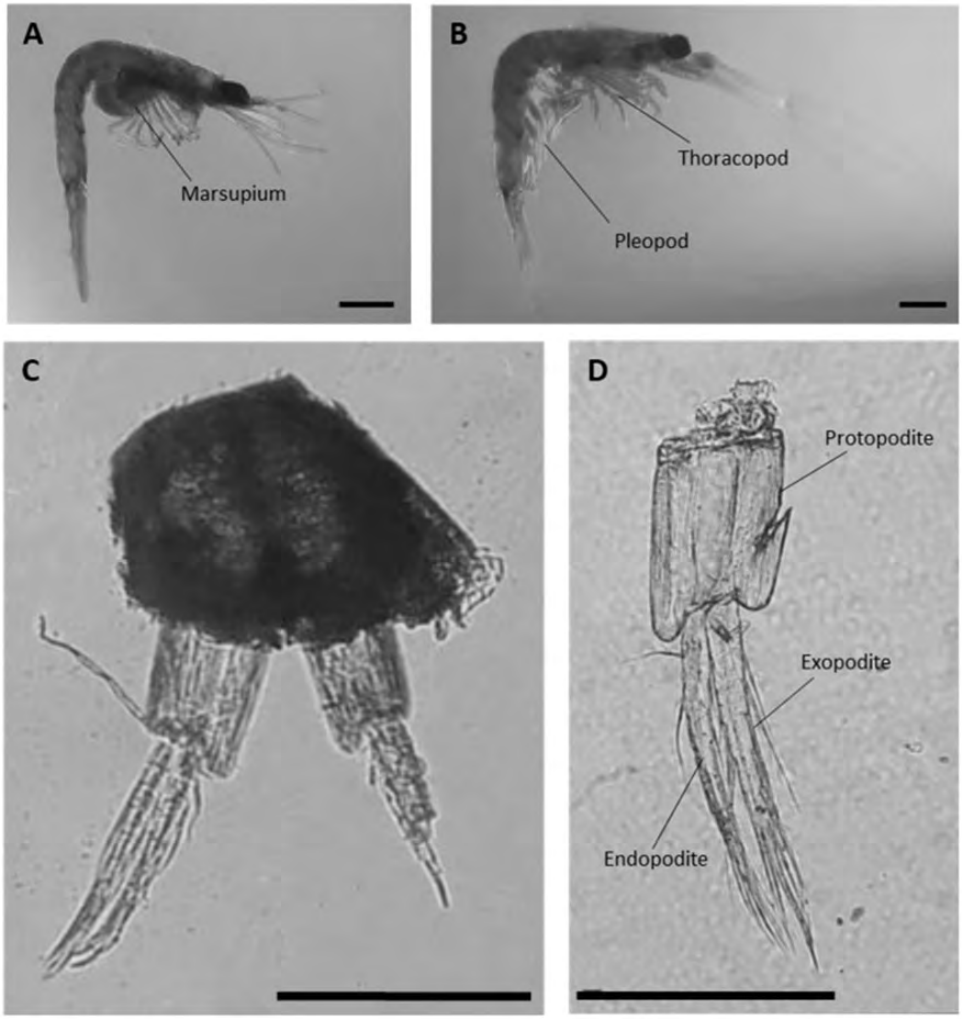

Fig. 1 *Americamysis bahia* morphology. Scale bars are 1 mm. (**A**) Adult female with marsupium. (**B**) Adult male with thoracopods and pleopods identified. (**C**) Transverse plane of the adult, male first abdominal segment with attached pleopods. The left pleopod is intact and the right pleopod has been damaged. (**D**) Adult, male pleopod from the third abdominal segment with protopodite, exopodite, and endopodite identified. Specimens were preserved in 37% by weight aqueous formaldehyde and photographed under a Wild M5A stereomicroscope.

are used for swimming (Meland et al. 2015). However, kinematic analyses of Mysida species reveal that these species rely on their thoracopods for swimming, which beat in a rostro-caudal ellipse on their cephalothorax (Laverack et al. 1977; Schabes and Hamner 1992). Even though Mysida may have pleopods, they rely on their thoracic appendages for swimming.

Americamysis bahia (order Mysida) is unusual because it uses its pleopods to swim, albeit occasionally. It is a hyperbenthic, subtropical species, primarily found in the Gulf of Mexico (Molenock 1969; Lussier et al. 1988; Johnson and Allen 2012). It is easy to culture in the laboratory and highly sensitive to toxins in the water column, making it a model organism for toxicity experiments (Lussier et al. 1988, 1999). *Americamysis bahia* have five pairs of pleopods on their abdomen that beat independently of each other, resulting in two ipsilateral metachronal cycles—one running along the left side, another running along the right side of the body. Further, *A. bahia* show pleopod sexual dimorphism within the species. Male pleopods are fully developed and female pleopods are reduced (Fig. 1). Males and females rely primarily on their thoracopods for propulsion, but males occasionally swim using their pleopods in addition to their thoracopods.

While previous studies have focused on system design and optimization for organisms using only one metachronal cycle, this paper will address how having two metachronal cycles comprising a metachronal stroke will alter swimming performance. In this paper when referring to metachrony in *A. bahia*,

a metachronal cycle refers to the five-paddle beat pattern on one side of the body and a metachronal stroke refers to the complete 10-paddle beat pattern of left and right cycles together. The metachronal gait and resulting swimming behavior in *A. bahia* is quantified to test the hypothesis that pleopod utilization results in different swimming behavior than thoracopod utilization. Two-cycle metachronal swimming in *A. bahia* is compared with one-cycle metachronal swimming in *E. superba* to test the hypotheses that multiple cycles (1) require different pleopod morphology, (2) maintain steadier swimming speeds, and (3) achieve similar nondimensional measurements of efficiency compared with a single-cycle design.

Materials and methods

Animal collection and maintenance

Experiments took place during the summers of 2018 and 2020. *Americamysis bahia* were ordered from Sachs System Aquaculture (St. Augustine, FL), and mailed via two-day shipping to the Georgia Institute of Technology (Atlanta, GA). Upon arrival, mysids were allowed to acclimate to room temperature before being transferred to a 36 L, 28 ppt, aerated, saltwater aquarium. Mysids were fed 36 h *Artemia* spp. nauplii twice daily, with bi-weekly 30% water changes. The tank was cleaned once per week. Under these conditions, healthy *A. bahia* cultures were maintained for up to 3 months.

Recording

For all experiments, 10 mysids were haphazardly selected from their housing tank and transferred to a 1 L, cubic, experimental tank. For thoracopod swimming experiments (2018), organisms were transferred directly from their housing tank to the experimental tank. For pleopod swimming experiments (2020), mysids were first transferred to a 3 × 3 pyrex spot plate and pleopod presence was verified underneath a Wild M5A stereomicroscope (Wild Heerbrugg, Switzerland) before being transferred to the experimental tank. The tank contained 28 ppt saltwater filtered through a Pall A/E glass fiber filter (1 μ-pore size). Animals were allowed a 30 min acclimation period in the experimental tank before recording began.

Unprovoked, free swimming mysid behavior was recorded by two orthogonally-positioned high-speed cameras (AOS PRI-X and AOS PRI-S; AOS Technologies AG, Baden-Daettwil, Switzerland), each with an AF Micro-Nikkor 60 mm f/2.8D lens at 500 fps, focused on the center of the tank, away from the walls to prevent boundary interactions. Cameras captured an active volume of 9.5 mL (2.3 cm × 2.3 cm × 1.8 cm). Each camera was backlit with an 850 nm dual voltage IR light (Super Circuits, Austin, TX) to prevent any phototactic response. The cameras were connected to a computer, where the experimenter watched live feeds. The cameras were manually triggered when an animal swam in the field of view, capturing the previous 1000 frames and recording the next 1000 frames. Recordings were saved for further analysis. Organisms were observed for 2 h periods before being switched for fresh animals, to ensure independent sampling. Digital calibration was accomplished by filming a 1 mm calibration wand in the active volume before each 30 min acclimation period began.

In 2018, experiments took place over 8 days, with a total of 14 2 h blocks. All mysid passes in front of both cameras were recorded regardless of the appendages used for swimming. One random pass from each block was selected for thoracopod swimming analysis, resulting in $n = 14$ instances of thoracopod swimming. In 2020, experiments took place over 4 days, with a total of 7 2 h blocks. These experiments differed from those in 2018 because mysids were pre-sorted to have pleopods and the recordings captured only pleopod swimming. One instance of pleopod swimming was randomly selected from each block. In tandem with six pleopod swimming instances recorded in 2018, there were $n = 13$ instances of pleopod swimming in *A. bahia*. The analyzed pleopod recordings featured at least one complete metachronal stroke that was in focus on one of the two cameras, with the organism being present in the view of the second camera, to allow for 3D reconstruction of appendage location.

Image analysis

Recordings were digitized using the DLTdv5 software (Hedrick 2008) for MATLAB. For thoracopod swimming analysis, the mysid's head and base of the telson were tracked on both cameras to extrapolate 3D kinematics. For pleopod swimming analysis, in addition to the head and the base of the telson, the sixth abdominal segment was tracked on both cameras, to determine if the telson angle (γ) affected swimming performance in *A. bahia*. Body length (BL) was measured as the distance from the organism's head to the base of the telson (Fig. 2).

On the camera that had the best lateral view of the organism, points where the pleopod met the body, midjoints between the protopod and exopodite, and pleopod tips were located in the digital image. Pleopod marker points were rotated into a three-dimensional position based on the three-dimensional

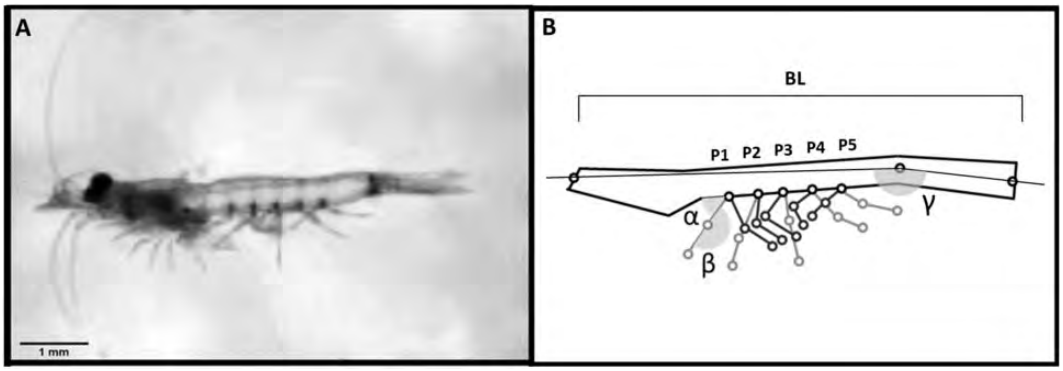

Fig. 2 *Americamysis bahia* digitization. (**A**) Image of a free swimming mysid with pleopods. (**B**) Digitization of a similarly positioned mysid, showing the points tracked, body length (BL), angle between the protopodite and the body (α), angle between the protopodite and the exopodite (β), and telson angle (γ). Pleopods are numbered such that P1 is the anterior-most and P5 is the posterior-most. Shading indicates ipsilateral members of the same metachronal cycle. P1–P5 in light gray, are in various stages of their power stroke, and P1–P5 in dark gray, are in various stages of their recovery stroke. Angles α and β are depicted on the P1 pleopod in its power stroke.

position of the head, sixth abdominal segment, and telson points, resulting in a 28-point digitization of the mysid. The angle the pleopod makes with its body (α) and angle between the protopod and the exopodite (β) was calculated from this data set (Fig. 2).

Instantaneous swimming speed was calculated by following the three-dimensional position of the head throughout the entire recording. Mean swimming speed was calculated from these points for the duration of the entire recording.

Recordings varied in the number of sequential metachronal strokes performed by the mysid, ranging from 1 to 6. For instances where there were multiple metachronal strokes within one recording, separate strokes were identified by the initiation of the first P5 power stroke captured on camera. This pleopod, whether on the left or the right side of the body, became the pleopod that differentiated between consecutive strokes, with one complete stroke lasting the duration between consecutive power strokes of this specific appendage. Stroke amplitude curves were calculated following the method of Murphy et al. (2011). Stroke amplitude data for each pleopod cycle were centered to begin at $t = 0$ s and standardized to the mean cycle period. Cubic spline functions were fit to each pleopod stroke, and 100 equally spaced points were calculated based on the fitted function. The individual curves were ensemble averaged to create the mean pleopod amplitude curves. Phase lag, stroke period, and cycle period were calculated from these curves.

Statistical analysis

Statistical analysis was performed in JMP Pro 15.0.0 (SAS Institute Inc., Cary, NC). Parametric comparisons were made when variables were each normally distributed (tested via Anderson–Darling test) and had equal variance (tested via Levene's test). Otherwise, non-parametric analysis between variables was performed. Data are reported as mean ± standard error. A first-order multivariate regression was performed to determine how *A. bahia* swimming speed depends on pleopod stroke amplitude, beat frequency, and phase lag.

Results

Thoracopod versus pleopod swimming

Americamysis bahia constantly beats its thoracopods to swim. Occasionally, the thoracopods are assisted by a brief series of metachronal strokes from its pleopods—the pleopods are never the sole propulsive appendage. Pleopod usage appeared random, and could not be associated with any stimulus. In 2018, when all instances of the mysid swimming in front of the cameras were recorded regardless of whether *A. bahia* used its pleopods or not, there were only six instances of *A. bahia* using its pleopods to swim out of 61 total passes. Based on these data, *A. bahia* use their pleopods approximately 10% of the time.

When using its pleopods, *A. bahia* achieves significantly greater swimming speeds (7.6 ± 0.7 BL/s, $n = 13$) compared with solely using its thoracopods (3.7 ± 0.6 BL/s, $n = 14$) (thoracopod swimming speeds not normally distributed, $P = 0.05$; two-Sample Wilcoxon Rank, $P = 0.001$) (Fig. 3). When using its thoracopods, the organism maintains a more stationary position in the water column by hovering in place, though it may also propel itself forward. In contrast, pleopods are utilized occasionally and only result in forward propulsion.

The angle the mysid made with the horizontal plane was quantified as body angle. A positive angle occurred when the organism's head was higher in the water column than its telson, and the organism was ascending, and a negative angle occurred when the organism was swimming deeper into the water column. There is no significant difference between the mean body angle the mysid has while swimming using its thoracopods ($21.4 \pm 6.0°$, $n = 14$) compared with while swimming with its pleopods ($9.5 \pm 7.8°$, $n = 13$) (thoracopod body angle not normally distributed, $P < 0.01$; two-Sample Wilcoxon Rank, $P = 0.17$). Though the mean body angle is positive for both propulsive approaches, the pleopod body angle data are skewed such that the mysid favors its pleopods over its thoracopods when diving.

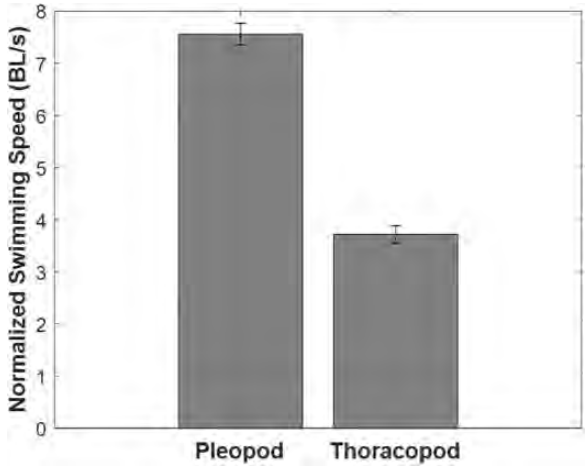

Fig. 3 Normalized swimming speeds for *A. bahia*. Mean normalized swimming speed and SE achieved when the mysid uses its pleopods ($n = 13$) or thoracopods ($n = 14$) to swim.

Pleopod metachrony in *A. bahia*

Figure 4 depicts α and β for one complete ideal stroke of the left and right cycles for *A. bahia*, beginning with the P5 power stroke in the left cycle. Left and right cycles are 180° out of phase with each other ($175.1 \pm 8.4°$, $n = 13$; one-sample *t*-test, $P = 0.58$). The pleopods beat at 13.8 ± 0.6 Hz ($n = 26$ cycles) in an adlocomotory fashion moving posteriorly to anteriorly within ipsilateral cycles. During the interval between consecutive P1–P5 power strokes in the same cycle, the opposite cycle initiates all five of its power strokes. The telson angle throughout the stroke is $162.7 \pm 5.2°$ ($n = 13$).

Phase lag was used to determine whether metachrony in *A. bahia* should be analyzed as one continuous 10-paddle stroke, or two concurrent ipsilateral five-paddle cycles. The time between initiations of power strokes between ipsilateral pleopods can be normalized by the duration of the entire stroke, resulting in a dimensionless parameter—phase lag (simplified for one ipsilateral cycle in Fig. 5A). Perfect metachrony occurs when phase lag is equal for each ipsilateral pair combination. For a

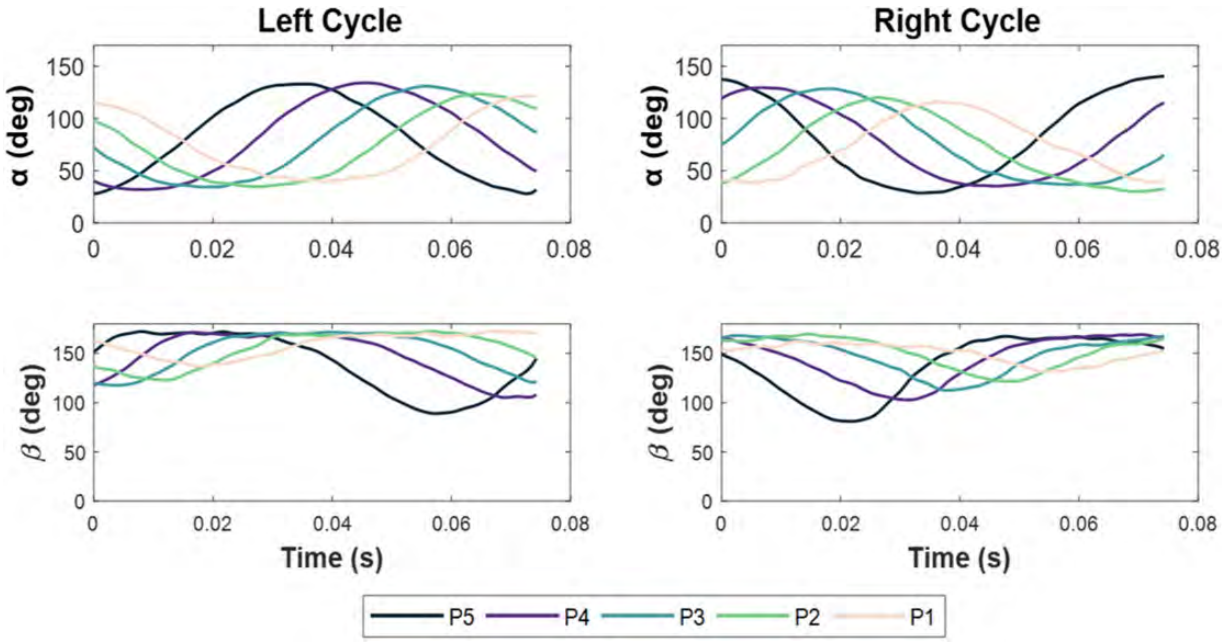

Fig. 4 Time standardized pleopod angles for ipsilateral cycles during one complete metachronal stroke. Angles for $n = 13$ cases were combined for each pleopod (following method in Murphy et al. 2011), represented in a different color, and time standardized to represent one ideal metachronal stroke.

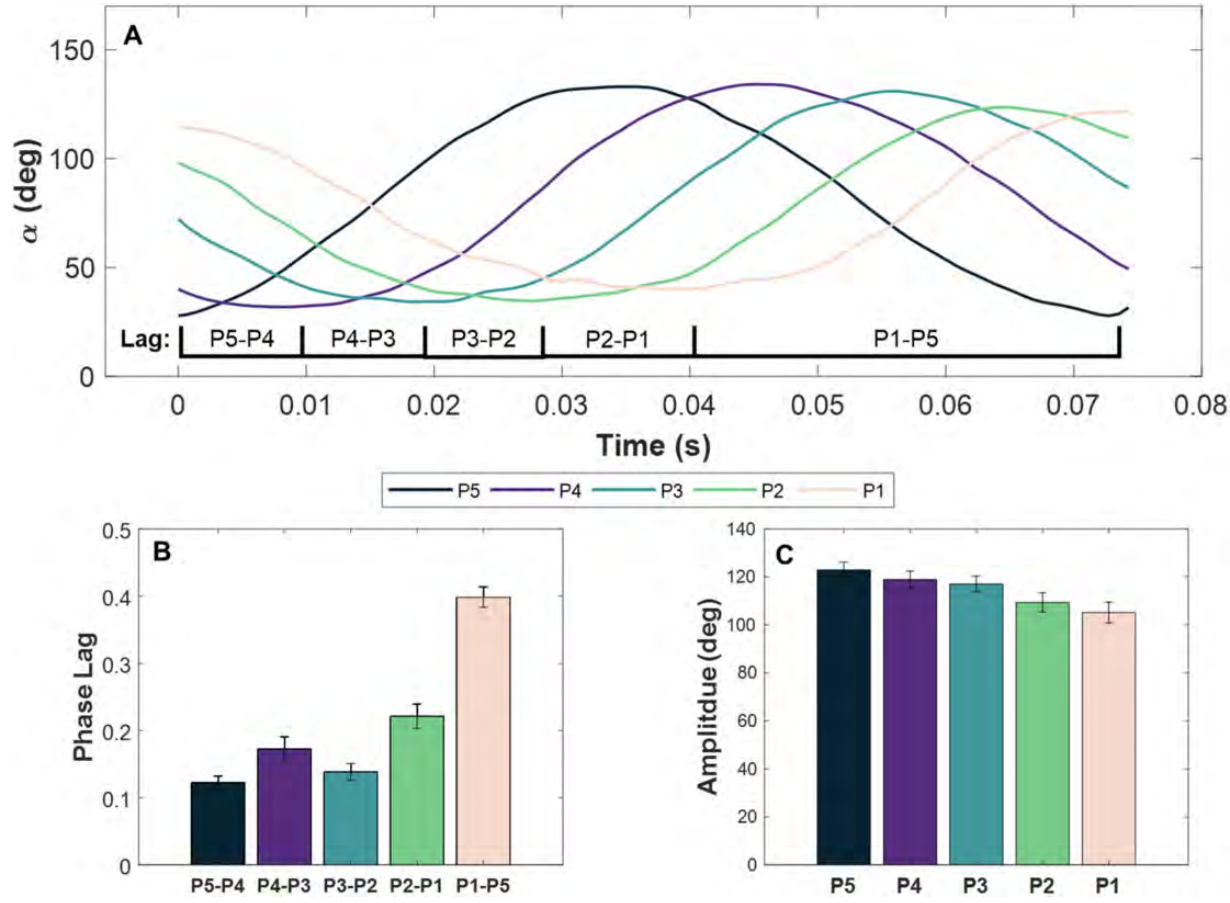

Fig. 5 Phase lag and amplitude in *A. bahia*. (**A**) Angle α for one ipsilateral cycle of *A. bahia* with individual brackets indicating the duration between adjacent pleopod power strokes. The entire bracket encloses the duration of the complete stroke. (**B**) The mean phase lag between adjacent pleopods, defined as the fraction of a full cycle between initiation of power strokes of adjacent pleopods. Phase lag data for pleopods on the same abdominal segment were combined to calculate mean ± SE ($n = 26$). (**C**) Stroke amplitudes for pleopods on the same abdominal segment combined to calculate mean ± SE stroke amplitude for each pleopod ($n = 26$).

10-paddle cycle, each phase lag is expected to equal one-tenth of the entire cycle's duration, resulting in an expected phase lag of 0.1. For a five-paddle cycle, each phase lag would last one-fifth of the cycle, for an expected phase lag of 0.2. To analyze the stroke as a continuous 10-paddle cycle, the stroke duration was calculated as the duration between two consecutive power strokes from the same P5 and the P1–P5 lag was calculated using power strokes from contralateral cycles. The mean phase lag was then calculated, pooling each ipsilateral pair combination for all 13 replicates, resulting in $n = 130$. The mean phase lag for *A. bahia* when analyzed as a 10-paddle stroke (0.16 ± 0.01, $n = 130$) is greater than the expected lag of 0.1 ($n = 130$, one-sample *t*-test, $P < 0.0001$). To analyze the stroke as two concurrent ipsilateral five-paddle cycles, left and right cycles were analyzed separately with P1–P5 phase lag calculated from the same cycle. Again, each ipsilateral pair combination was pooled for the mean calculation, resulting in $n = 130$. The mean phase lag for each ipsilateral pair spacing when the stroke is analyzed as two concurrent five-paddle cycles (0.21 ± 0.01, $n = 130$) closely agrees to the ideal 0.2 phase lag expected from a five-paddle metachronal stroke ($n = 130$, one-sample *t*-test, $P = 0.71$). Therefore, metachrony in *A. bahia* was analyzed as though the organism's complete stroke is comprised of two concurrent ipsilateral five-paddle cycles.

To determine how to best pool data, pleopod-specific variables, including pleopod tip speed, stroke amplitude, beat frequency, and phase lag were compared between corresponding contralateral appendages using a random complete block ANOVA, with the individual serving as a block. Pleopod length was assumed to be the same for left and right pleopods on the same abdominal segment. Pleopod tip speed ($P = 0.11$), stroke amplitude ($P = 0.06$), and β amplitude ($P = 0.24$) could be pooled per abdominal segment, resulting in $n = 26$ observations for these variables. Phase lag between ipsilateral pleopods varied between cycles ($P < 0.0001$), but was

assumed to be a consequence of turning and was pooled for mean calculations. Cycle beat period was calculated based on the time between consecutive P5 power strokes in the same ipsilateral cycle, resulting in two frequencies, one per cycle. For each pass, there was no significant difference between cycle frequencies for the left and right sides ($P = 0.34$), and cycle frequencies were combined for each pass, resulting in $n = 26$ beat frequencies.

Although the mean phase lag of all ipsilateral pairs is 0.21, there is variation between phase lags from different ipsilateral pairs. The P2–P1 (0.23 ± 0.02, $n = 26$) and P1–P5 (0.42 ± 0.02, $n = 26$) lags are greater than 0.2 ($p_{P2–P1} = 0.05$, $n = 26$; $p_{P1–P5} < 0.0001$, $n = 26$), while P3–P2 (0.12 ± 0.01, $n = 26$) and P5–P4 (0.10 ± 0.01, $n = 26$) are less than 0.2 ($p_{P3–P2} < 0.0001$, $n = 26$; $p_{P5–P4} < 0.0001$, $n = 26$). Only the P4–P3 lag is not significantly different from 0.2 (0.17 ± 0.02, $P = 0.2$, $n = 26$). The greatest inter-limb phase lag occurs between P1 and the initiation of the next cycle in the following P5 power stroke, corresponding to the time when the opposite cycle is in its set of power strokes (Fig. 5B).

Stroke amplitude, calculated from α, varied between pleopods ($F = 3.8$, $P < 0.01$) (Fig. 5C). The only significant difference between stroke amplitudes occurred between P5 ($122.9 \pm 3.2°$, $n = 26$) and P1 ($105.2 \pm 4.4°$, $n = 26$) (Tukey–Kramer HSD, $P < 0.01$). The amplitudes for P2 ($109.4 \pm 4.1°$, $n = 26$), P3 ($117.0 \pm 3.3°$, $n = 26$), and P4 ($118.9 \pm 3.5°$, $n = 26$) were not different compared with those for any other pleopod.

Americamysis bahia pleopods have significantly different lengths in relation to their position on their body ($F = 3.58$, $P < 0.01$). P1 is 0.66 ± 0.02 mm, P2 is 0.69 ± 0.02 mm, P3 is 0.70 ± 0.02 mm, P4 is 0.68 ± 0.02 mm, and P5 is 0.61 ± 0.02 mm in length ($n_{P1} = n_{P2} = n_{P3} = n_{P4} = n_{P5} = 26$). P5 is significantly shorter than both P2 and P3 (Tukey–Kramer HSD, $p_{P5–P2} = 0.02$, $p_{P5–P3} = 0.01$). The rest of the pleopods are similar in length. The spacing between appendages can be calculated as the distance between adjacent appendages (G) normalized by the appendage length (L). The mean G/L ratio between pleopods is 0.46 ± 0.01.

Increasing swimming speed

A multivariate regression was used to determine how stroke amplitude, beat frequency, and phase lag affect swimming speed. Stroke amplitude data were combined into one variable, mean stroke amplitude, for analysis due to high correlation of amplitude among appendages (Supplementary Table S1) and to prevent collinearity in the final model. Phase lag data were not as highly correlated as stroke amplitude data and were analyzed independently in the model (Supplementary Table S2). Multiple correlations were analyzed to verify significant relationships between model inputs and normalized swimming speed, and only parameters with significant relationships were included in the final model.

Two models were analyzed to determine how stroke amplitude, beat frequency, and various phase lags contribute to swimming speed in *A. bahia*. The results of both models, as well as their zero-order relations with swimming speed are summarized in Table 1. The first model includes all variables that had a significant linear relationship with normalized swimming speed. Though this model shows a significant relationship between the input terms and swimming speed ($R^2 = 0.75$, $R_{adj}{}^2 = 0.58$, $F = 4.30$, $P = 0.04$), the variance inflation factor (VIF) is greater than 5 for P5–P4 lag in this calculation, suggesting collinearity is present in the model. The second model removes P5–P4 lag and the collinearity decreases. This model accounts for 62% of the overall variance ($R^2 = 0.75$, $R_{adj}{}^2 = 0.62$, $F = 5.98$, $P = 0.02$). Stroke amplitude is the only parameter to significantly contribute to this model ($P = 0.05$).

Discussion

Consequences of multiple cycles

Morphology

The most defining feature of metachrony in *A. bahia* is the number of paddles used in one stroke. Euphausiids' and decapods' contralateral pleopods are connected with a retinaculum ensuring they beat at the same time in a metachronal stroke with three to five paddles. Mysid shrimp lack a retinaculum, allowing their pleopods to beat independently (Grams and Richter 2021). *Americamysis bahia* employs two simultaneous, five-paddle metachronal cycles—one running along the left side, the other along the right side of the body—effectively using 10 total paddles in its metachronal stroke instead of 5. Having more paddles in a metachronal stroke at this Reynolds number is beneficial to *A. bahia* (mean Re $= 170 \pm 20$). At Reynolds numbers of 100, efficiency, measured as time-averaged fluid flux to time-averaged power supplied to the fluid, increases with the number of paddles, only operating at 90% efficiency with four paddles, and reaching maximum efficiency at eight paddles and beyond (Granzier-Nakajima et al. 2020).

Pleopod structure differs between *A. bahia* and *E. superba*. In *A. bahia*, the protopodite is $48 \pm 2\%$

Table 1 Zero-order correlation and regression results for two models employed to predict swimming speed

			Model 1			Model 2		
Term	Zero-order r	*P*	Standardized coefficient	*P*	VIF	Standardized coefficient	*P*	VIF
Intercept	–	–	0.00	0.31	–	0.00	0.24	–
Amplitude	0.63	**0.02**	0.57	0.21	4.72	0.43	**0.05**	1.17
Frequency	0.64	**0.02**	0.20	0.44	1.74	0.23	0.32	1.53
P5–P4 lag	−0.68	**0.01**	0.18	0.74	6.58	–	–	–
P4–P3 lag	−0.45	0.12	–	–	–	–	–	–
P3–P2 lag	−0.61	**0.03**	−0.35	0.34	3.46	−0.26	0.30	1.75
P2–P1 Lag	0.64	**0.01**	0.28	0.31	1.83	0.26	0.30	1.80
P1–P5 Lag	0.48	0.10	–	–	–	–	–	–

Significant relationships with swimming speed are bolded.

the length of the entire pleopod, whereas in *E. superba*, the protopodite is 41 ± 2% the length of the entire pleopod. In *A. bahia*, the protopodite, as the upper section of the pleopod that connects the appendage to the body, houses more appendage musculature than the more distal exopodite and endopodite, which may be where *A. bahia* derive the power for their stroke (Hessler 1985). *Euphausia superba* fan their exopodite and endopodite on their pleopods at an angle of 80° to increase the surface area of their paddles and increase thrust (Murphy et al. 2011). In this study, though the distal segment of the pleopods has an exopodite and endopodite, they were not observed to fan out.

Gait kinematics

Though pleopod usage is infrequent, due to our inability to associate pleopod usage with any specific stimuli, pleopod swimming in *A. bahia* appears to be a general swimming behavior. It is assumed to be a sustained swimming behavior rather than an escape response even though it is only observed for short periods of time, and as such, warrants comparison to other organisms with a similar body plan that use their pleopods to swim—primarily *E. superba* and the mysid *G. ingens*.

An important question for *A. bahia* is whether swimming speed is related to stroke amplitude and frequency, as these parameters are strong predictors for *E. superba* swimming speed (Murphy et al. 2011). A first-order multivariate regression was employed for *A. bahia* swimming kinematics to determine which stroke parameter is most responsible for dictating swimming speed. Most parameters expected to predict swimming speed showed similar, low levels of correlation with swimming speed in *A. bahia*. Stroke amplitude, beat frequency, P5–P4 phase lag, P3–P2 phase lag, and P2–P1 phase lag were all significant zero-order predictors. Of these, P5–P4 phase lag was highly correlated with the other predictors and could be encapsulated in those variables. Of the final parameters used in the first-order multivariate regression, stroke amplitude was the only significant predictor in the model, suggesting that stroke amplitude has the strongest effect on swimming speed in *A. bahia* (Table 1). In the final model, increasing frequency, decreasing P3–P2 lag, and increasing P2–P1 lag all have a similar weight on swimming speed, reflected in similar standardized coefficients.

When using their pleopods, *A. bahia* swim in a horizontal orientation (mean body angle = 9.5 ± 7.8°, $n = 13$) at speeds greater than 2 BL/s, which matches the qualifications for fast forward swimming defined in Murphy et al. (2011). *Euphausia superba*, in contrast, have much more variability in their metachrony, evident in the different swimming behaviors they can achieve. They can hover, swim fast forward, or swim upside down, differentiable by the organism's swimming speed and orientation (Murphy et al. 2011).

Americamysis bahia have less variability in stroke amplitude compared with *E. superba* and can achieve greater normalized swimming speeds (Fig. 6). The primary reason for the difference is the swimming styles of these organisms. *Euphausia superba* swims only using its pleopods and achieves speeds less than 2 BL/s by decreasing its stroke amplitude. In contrast, *A. bahia* never swims less than 2 BL/s when using its pleopods—it achieves these slower swimming speeds when using its thoracopods.

Above the 2 BL/s threshold, *E. superba* transitions to increasing its speed by increasing beat frequency, rather than stroke amplitude (Murphy et al. 2011). *Americamysis bahia* also increase beat frequency to swim faster, though this relationship is not as strong as it is in *E. superba* (Fig. 7A). The hyperbenthic mysid *G. ingens*, which also uses two ipsilateral metachronal cycles, never swims faster than 2 BL/s (Cowles et al.

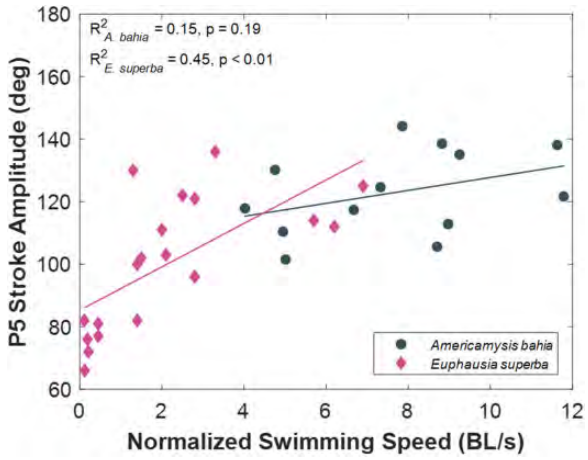

Fig. 6 P5 stroke amplitude and normalized swimming speed for *A. bahia* and *E. superba* (Murphy et al. 2011).

1986). While this variability in attainable speeds may be attributed to differences in experimental conditions between the three studies, if a logistic growth curve is fit to these data, a maximum beat frequency for attainable speeds using metachrony occurs at approximately 15 Hz ($R^2 = 0.88$), indicating an upper limit to stroke frequency in metachrony. Even though these three species swim with their pleopods at vastly different normalized speeds, come from different environments, and exist at different Reynolds numbers, they all achieve similar speeds, between 0 and 10 cm/s, indicating a practical range of speeds in which sustained metachrony is an effective approach to aquatic locomotion (Fig. 7B).

Smoothness of swimming

Swimming speeds in *A. bahia*, while they may fluctuate over the duration of an entire stroke, show no periodic increases that have been associated with specific power strokes in other organisms (Fig. 8). When *E. superba* hover, their speed shows periodic increases corresponding to their P3 power stroke, which is their longest paddle (Murphy et al. 2013). Remipedes also show periodic speeds, with increased speeds corresponding to their longest paddles (Kohlhage and Yager 1994). *Americamysis bahia* have no significantly long appendage. Even though P3 is the longest pleopod, there is no spike in speed correlated to a P3 power stroke in *A. bahia*.

The more constant speed may be a result of *A. bahia* having more paddles in its metachronal stroke than *E. superba*. Though metachrony in *A. bahia* is comprised of two, five-paddle cycles, the entire stroke consists of 10 paddles operating independently of each other, twice as many paddles compared with *E. superba*. Each power stroke contributes some amount of thrust to the resulting motion. As the number of paddles in a stroke increases, the time between each power stroke decreases, allowing for a more constant output of thrust and less impulse from any specific paddle. Organisms with only one set of paddles, like daphniids (Skipper et al. 2019) and juvenile *Artemia* sp. (Williams 1994), have sharp periodic speed graphs, corresponding to their power stroke. As the number of paddles in a stroke increases, these impulses occur more frequently, and should result in smoother swimming. *Americamysis bahia*'s more constant speed may be a result of not having a significantly long appendage, or a greater number of paddles used in its metachronal stroke compared with euphausiids.

Nondimensional characterization

The challenge of comparing variables across different metachronal designs highlights the need for nondimensional comparisons, which allow for

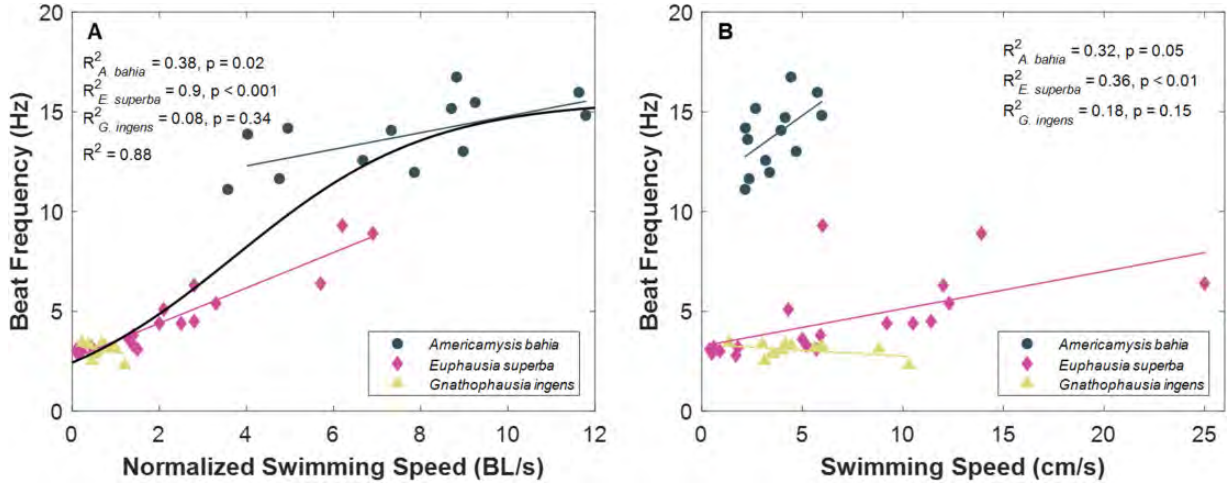

Fig. 7 Beat frequency and swimming speed for *A. bahia*, *E. superba* (Murphy et al. 2011), and *G. ingens* (Cowles et al. 1986). (**A**) Frequency plotted against normalized swimming speed. (**B**) Frequency plotted against swimming speed.

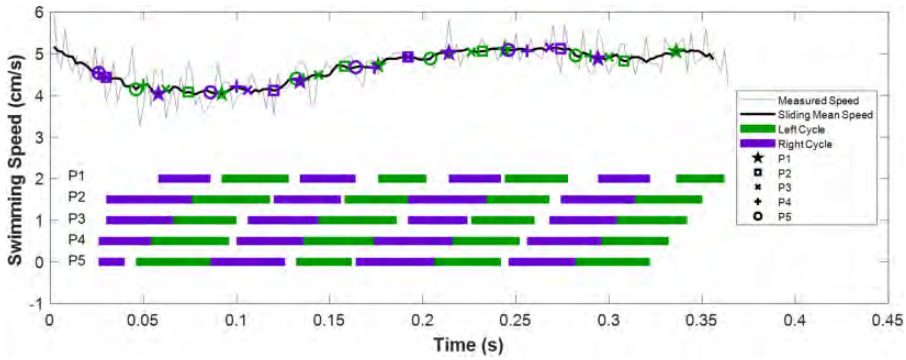

Fig. 8 Sample swimming speed and power stroke synchrony. Data were collected from one pass containing four complete metachronal cycles in *A. bahia*. Swimming speed data consist of the measured speed in light gray, and a sliding mean value, taken over 0.02 s, in black. The bottom portion of the figure depicts the timing and duration of the power strokes for each pleopod, and the bars are color-coded by cycle. Marker points are depicted on the sliding mean swimming speed curve that corresponds to the initiation of respective pleopod power strokes. The color of these points corresponds to the cycle, and the shape of the points corresponds to the pleopod.

generalizations about relationships to be made across different length scales. Table 2 summarizes important nondimensional parameters in crustaceans with different numbers of cycles per stroke, numbers of paddles per cycle, and Reynolds numbers.

There are two variants of the Reynolds number to consider when looking at metachronal motion. The first is the whole-body Reynolds number (Re_{body}), calculated using the BL and the resulting swimming speed of the organism. The second variant is the Reynolds number of the pleopod (Re_{pleo}) that uses the length of the pleopod (L_{pleo}) and the maximum speed of the pleopod tip during the power stroke (U_{pleo}), which can be estimated as

$$U_{pleo} = \pi f \theta L_{pleo}, \tag{2}$$

where f is the stroke frequency and θ is the stroke amplitude in radians. The whole-body Reynolds number for *A. bahia* is 170 ± 20 ($n = 13$) and the Reynolds number of the pleopods is 40 ± 3 ($n = 13$). There is a factor of roughly four difference between the pleopods and the body, firmly putting the pleopods in a drag-based regime. This nearly order-of-magnitude difference between pleopod and whole-body Reynolds number is consistent across other species.

The Strouhal number, defined as

$$\mathrm{St} = \frac{fA}{V}, \tag{3}$$

where f is the frequency, A is the arc length of the flapping appendage estimated as $2L_{pleo}\sin(\text{amplitude}/2)$, and V is the resulting velocity, is a fluid dynamics parameter used to describe flow with an oscillating component. It represents the ratio of unsteady effects to inertial effects. At higher St, oscillations dominate in the flow, and at low St, the oscillations are swept by the moving fluid. Strouhal numbers between 0.2 and 0.4 result in the highest propulsive efficiency of a flapping airfoil (Triantafyllou et al. 1993), and this efficient Strouhal number range is observed in many organisms that flap or paddle (Taylor et al. 2003). The mean St for *A. bahia* is 0.5 ± 0.04 ($n = 13$, Table 2), which falls just outside of this efficient range.

In swimming fish, St varies with speed. At low speeds (<1 BL/s), Strouhal numbers are highly variable, and have been recorded as low as 0.1 and as high as 0.9. As speed increases, these values converge to the more efficient value of St = 0.3 (Saadat et al. 2017). This trend also exists in *A. bahia* (Fig. 9). Although *A. bahia*'s mean St is greater than the optimal range 0.2–0.4, as its speed increases, its St decreases and falls into the efficient range at speeds above approximately 9 BL/s. *Americamysis bahia* pleopod motion appears tuned to achieve fast speeds.

The advance ratio, defined as

$$J = \frac{V}{2\theta f L_{pleo}}, \tag{4}$$

where θ is the stroke amplitude in radians, is another nondimensional measure of efficiency (Walker 2002; Murphy et al. 2011). It is the ratio of the resulting body speed to appendage speed. For large advance ratios ($J \geq 1$), the organism moves at the same speed, or faster than its appendages. For small advance ratios, the appendages move quicker than the body.

Many organisms with one set of appendages have an advance ratio between 0.1 and 0.6 (Walker 2002), indicating that the resulting speed of the body is less than that of the appendages. However, with multi-appendage swimmers, J is often greater than 1, indicating that the legs are moving at the same speed or slower than the body. If it is assumed that each

Table 2 Metachronal characterization of four crustaceans

Species	Contralateral appendage symmetry	Paddles per cycle	BL (cm)	Swimming speed (BL/s)	Stroke frequency (Hz)	Re_{body}	Re_{pleo}	St	J	J_n	Reference
Americamysis bahia	no	5	0.47 ± 0.02	7.6 ± 0.7	13.8 ± 0.6	170 ± 20	40 ± 3	0.50 ± 0.04	0.9 ± 0.05	0.09 ± 0.01	This paper
Gnathophausia ingens	no	13	6–12	0.7	3.12	2000	900	0.82	0.5	0.02	Hessler (1985), Cowles et al. (1986)
Euphausia superba	yes	5	3.5 ± 1.3	4.0 ± 1.9	6.2 ± 2.0	2000	800	0.50	1.1–1.5	0.2–0.3	Murphy et al. (2011)
Odontodactylus havanensis	yes	5	3.5–6.4	20–40	17.0	50,000	5000	0.2	2.1	0.4	Campos et al. (2012)

Re_{body} and Re_{pleo} are variants of Equation (1). St calculated from Equation (3), J calculated from Equation (4), and J_n from Equation (5). *Euphausia superba* data include only fast-forward swimming.

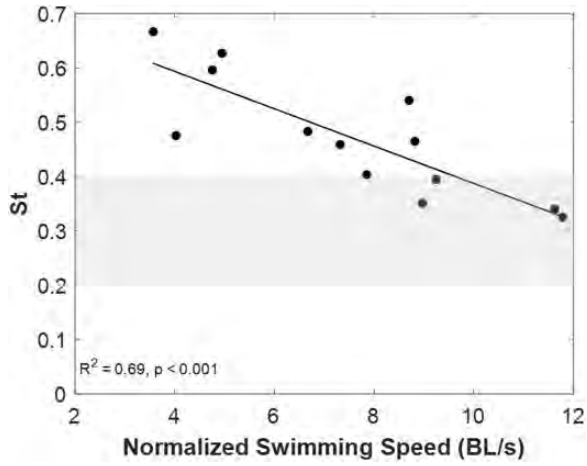

Fig. 9 Strouhal number (St) decreases with normalized swimming speed for *A. bahia*. The shaded gray region highlights the efficient Strouhal number range of 0.2–0.4 as documented by Taylor et al. (2003).

paddle in a stroke equally contributes to the total thrust, the advance ratio for multi-appendage swimmers can be normalized by the number of paddles in a metachronal stroke

$$J_n = \frac{V}{2\theta f L_{\text{pleo}} n}, \tag{5}$$

where n is the number of paddles, then J_n values for multi-appendage species are similar to the 0.1–0.6 range observed in organisms with one appendage (Walker 2002; Murphy et al. 2011).

For *A. bahia*, J_n (0.09 ± 0.01, $n = 13$) falls just outside the expected range of 0.1–0.6 (Table 2). The appendage tip is moving faster than the resulting body speed. However, J_n increases with swimming speed, and it reaches J_n of 0.1 at approximately 9 BL/s (Fig. 10). The other two-cycle mysid, *G. ingens*, also has an extremely low J_n of 0.02, and it swims at speeds less than 2 BL/s (Table 2). Small J_n ratios at low speeds in mysids indicate that employing multiple metachronal cycles is relatively ineffective at low speeds. Together, trends with St and J_n and swimming speed suggest that dual ipsilateral metachrony is effective at speeds greater than 9 BL/s in *A. bahia*.

When to use pleopods

Pleopod stroking results in fast forward swimming and in speeds greater than when the organism uses its thoracopods alone to swim. However, it remains unclear what acts as a cue for *A. bahia* to swim using its pleopods. All experiments were performed such that there was no stimulus exerted on the tank from the experimenter. It is possible that heating in the laboratory or

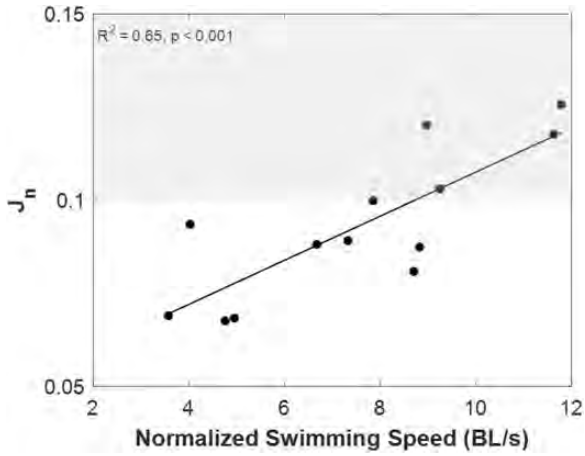

Fig. 10 Normalized advance ratio (J_n) increases with normalized swimming speed for *A. bahia*. The shaded gray region highlights the expected range of J_n values for one-paddle swimmers of 0.1–0.6 as documented in Walker (2002).

ventilation may have provoked pleopod swimming, but this was not noticed. This study also cannot say how infrequent this behavior is. The estimate of 10% does not take into account the sex of the individuals recorded. In 2020, the experimental design was set up such that only recordings of pleopod utilization were captured. Additionally, *A. bahia* doesn't necessarily streamline itself in order to go faster, as has been observed in *E. superba* (Murphy et al. 2011), the body angles for thoracopod swimming and pleopod swimming do not differ. Pleopod swimming allows the organism to travel in the same direction that thoracopod swimming does, though it shows an insignificant bias to using its pleopods while diving.

Study limitations

In these observations, *A. bahia* beat their pleopods for short amounts of time, only completing 2.5 ± 0.4 ($n = 13$) strokes per recording. Because of the limited number of strokes, pleopod beating in *A. bahia* results in quick bursts of speed. However, if more strokes were to occur, the mysid may show greater maneuverability. For example, if the cycle frequencies were different within the stroke, pleopod usage could result in an imbalance of force turning the animal in the direction of the slower cycle. Differences in cycle beat frequencies corresponding to a turn were not observed, though the duration of most of these recordings was short, only 0.3 ± 0.04 s, making it difficult to accurately quantify the organisms' trajectory. Additionally, similar ipsilateral phase lags differed between concurrent cycles, but due to the short time series, these data were pooled per abdominal segment. Changing the phase lag between ipsilateral paddles affects the swimming speed of the organism, but no attempts have been made to relate phase lag to measurements of trajectory.

This study focused on the kinematics of metachrony, and due to the relative complexity of the creature, some measurements were difficult. The motion of a pleopod throughout the stroke is not fully defined. Images show that *A. bahia* pleopods have an exopodite and endopodite on the distal segment of their pleopod, but the fanning of these segments was not visible in the recordings. The extent to which *A. bahia* fan out to increase the surface area of the stroke, and how this potential fanning compares to *E. superba* that are not space-limited by the presence a contralateral appendage in a separate cycle remains unclear.

This study also focuses on the swimming kinematics of *A. bahia*. Though the corresponding fluid mechanics are speculated about, no flow measurements were taken. Further research into the hydrodynamics of dual ipsilateral metachrony would provide more insight as to why this is effective at faster speeds, and why only some mysid species use pleopods to swim.

Conclusion

Americamysis bahia beat their 10 pleopods independently, resulting in two concurrent ipsilateral metachronal cycles. Pleopod usage in *A. bahia* results in faster swimming than thoracopodal swimming and greater normalized swimming speeds than the one-cycle euphausiid, *E. superba*. There is no apparent relationship between cyclic increases in swimming speed with the power stroke of any particular limb, suggesting that more legs result in smoother swimming. Additionally, *A. bahia* does not use its pleopods to swim at speeds less than 2 BL/s, and analysis of nondimensional parameters suggests that multiple cycles are inefficient at speeds less than 9 BL/s.

Funding

This work was supported by a grant from the National Science Foundation [CTS 1706007 to D.R.W. and J.Y.].

Data availability statement

Further data supporting this study are available upon request to the authors.

Supplementary data

Supplementary data are available at *ICB* online.

References

Alben S, Spears K, Garth S, Murphy D, Yen J. 2010. Coordination of multiple appendages in drag-based swimming. J R Soc Interface 7:1545–57.

Anderson EJ, Grosenbaugh MA. 2005. Jet flow in steadily swimming adult squid. J Exp Biol 208:1125–46.

Ayancik F, Fish FE, Moored KW. 2020. Three-dimensional scaling laws of cetacean propulsion characterize the hydrodynamic interplay of flukes' shape and kinematics. J R Soc Interface 17:20190655.

Campos EO, Vilhena D, Caldwell RL. 2012. Pleopod rowing is used to achieve high forward swimming speeds during the escape response of *Odontodactylus havanensis* (Stomatopoda). J Crust Biol 32:171–9.

Cheer AYL, Koehl MAR. 1987. Paddles and rakes: fluid flow through bristled appendages of small organisms. J Theor Biol 129:17–39.

Colin SP, Costello JH, Sutherland KR, Gemmell BJ, Dabiri JO, Du Clos KT. 2020. The role of suction thrust in the metachronal paddles of swimming invertebrates. Sci Rep 10:17790.

Costello JH, Colin SP, Gemmell BJ, Dabiri JO, Sutherland KR. 2015. Multi-jet propulsion organized by clonal development in a colonial siphonophore. Nat Commun 6:1–6.

Cowles DL, Childress JJ, Gluck DL. 1986. New method reveals unexpected relationship between velocity and drag in the bathypelagic mysid *Gnathophausia ingens*. Deep Sea Res 33:865–80.

DeMont ME, Gosline JM. 1988. Mechanics of jet propulsion in the hydromedusan jellyfish, *Polyorchis penicillatus* II. Energetics of the jet cycle. J Exp Biol 134:333–45.

Drucker EG, Jensen JS. 1996. Pectoral fun locomotion in the striped surfperch I. Kinematic effects of swimming speed and body size. J Exp Biol 199:2235–42.

Fish FE, Lauder GV. 2006. Passive and active flow control by swimming fishes and mammals. Annu Rev Fluid Mech 38:193–224.

Ford MP, Santhanakrishnan A. 2020. On the role of phase lag in multi-appendage metachronal swimming of euphausiids. Bioinspir Biomim published online (doi: 10.1088/1748-3190/abc930).

Fulton CJ, Johansen JL, Steffensen JF. 2013. Energetic extremes in aquatic locomotion by coral reef fishes. PLoS ONE 8:e54033.

Grams M, Richter S. 2021. Locomotion in *Anaspides* (Anaspidacea, Malacostraca)—insights from a morpho-functional study of thoracopods with some observations on swimming and walking. Zoology 144:125883.

Granzier-Nakajima S, Guy RD, Zhang-Molina C. 2020. A numerical study of metachronal propulsion at low to intermediate Reynolds numbers. Fluids 5:86–15.

Hedrick TL. 2008. Software techniques for two- and three-dimensional kinematic measurements if biological and biomimetic systems. Bioinspir Biomim 3:034001.

Hessler RR. 1985. Swimming in crustacea. Earth Environ Sci Trans R Soc Edinb 76:115–22.

Johnson WS, Allen DM. 2012. Zooplankton of the Atlantic and Gulf Coasts: A Guide to their Identification and Ecology. Baltimore (MD): The John Hopkins University Press.

Kim D, Gharib M. 2011. Characteristics of vortex formation and thrust performance in drag-based paddling propulsion. J Exp Biol 214:2283–91.

Kohlhage K, Yager J. 1994. An analysis of swimming in remipede crustaceans. Phil Trans R Soc Lond B 346:213–21.

Laverack MS, Neil DM, Robertson RM. 1977. Metachronal exopodite beating in the mysid *Praunus flexuosus*: a quantitative analysis. Proc R Soc Lond B 198:139–54.

Lussier SM, Kuhn A, Chammas MJ, Sewall J. 1988. Techniques for the laboratory culture of *Mysidopsis* species (Crustacea: Mysidacea). Environ Toxicol Chem 7:969–77.

Lussier SM, Kuhn A, Comeleo R. 1999. An evaluation of the seven-day toxicity test with *Americamysis bahia* (formerly *Mysidopsis bahia*). Environ Toxicol Chem 18:2888–93.

Meland K, Mees J, Porter M, Wittmann KJ. 2015. Taxonomic review of the orders Mysida and Stygiomysida (Crustacea, Pericarida). PLoS ONE 10:e0124656.

Molenock J. 1969. *Mysidopsis bahia*, a new species of mysid (Crustacea: Mysidacea) from Galveston Bay, Texas. Tulane Stud Zool Bot 15:113–6.

Murphy DW, Webster DR, Kawaguchi S, King R, Yen J. 2011. Metachronal swimming in Antarctic krill: gait kinematics and system design. Mar Biol 158:2541–54.

Murphy DW, Webster DR, Yen J. 2013. The hydrodynamics of hovering in Antarctic krill. Limnology and Oceanography: Fluids and Environments3:240–55.

Quetin LB, Childress JJ. 1980. Observation on the swimming activity of two bathypelagic mysid species maintained at high hydrostatic pressures. Deep Sea Res 27:383–91.

Ross RM, Quetin L. 2000. Reproduction in Euphausiacea. In: Everson I, editor. Krill: biology, ecology, and fisheries. Oxford: Blackwell Publishing. p. 150–81.

Saadat M, Fish FE, Domel AG, Di Santo V, Lauder GV, Haj-Hairiri H. 2017. On the rules for aquatic locomotion. Phys Rev Fluids 2:1–12.

Schabes M, Hamner W. 1992. Mysid locomotion and feeding: kinematics and water-flow patterns of *Antarctomysis* sp., *Acanthomysis sculpta*, and *Neomysis rayii*. J Crust Biol 12:1–10.

Skipper AN, Murphy DW, Webster DR. 2019. Characterization of hop-and-sink daphniid locomotion. J Plankton Res 41:142–53.

Tattersall WM, Tattersall OS. 1951. The British Mysidacea. London (UK): Bartholomew Press.

Taylor GK, Nudds RL, Thomas ALR. 2003. Flying and swimming animals at a Strouhal number tuned for high power efficiency. Nature 425:707–11.

Triantafyllou GS, Triantafyllou MS, Grosenbaugh MA. 1993. Optimal thrust development in oscillating foils with application to fish propulsion. J Fluids Struct 7:205–24.

Vogel S. 2013. Thrust for flying and swimming. In: Press PU, editor. Comparative biomechanics: life's physical world. Princeton (NJ): Princeton University Press. p. 251–70.

Walker JA. 2002. Functional morphology and virtual models: physical constraints on the design of oscillating wings, fins, legs, and feet at intermediate Reynolds numbers. Integr Comp Biol 42:232–42.

Williams TA. 1994. A model of rowing propulsion and the ontogeny of locomotion in *Artemia* larvae. Biol Bull 187:164–73.

Yen J. 2000. Life in transition: balancing inertial and viscous forces by planktonic copepods. Biol Bull 198:213–24.

Zhang C, Guy RD, Mulloney B, Zhang Q, Lewis TJ. 2014. Neural mechanism of optimal limb coordination in crustacean swimming. Proc Natl Acad Sci USA 111:13840–5.